

Petrology and Geochemistry Jurassic Granitoid Intrusive, West Esfahan

¹Marziyeh Mehranfar, ²Nasr Esfahani Alikhan, ³Zohreh Hossein Mirzaee Beni

¹Petrology Department, Islamic Azad University, Khorasgan Branch, Isfahan, Iran.

²Department of Geology, Islamic Azad University (IAU), Isfahan branch (Khorasgan), Iran.

³young research club, Khorasgan branch, Islamic Azad University, Isfahan, Iran.

Abstract: The granitoid intrusive is located in W Isfahan and S Tiran and is a part of Sanandaj- Sirjan structural zone in Shahrekord-Dehsard. This plutonic is probably of middle Jurassic age at before cretaceous and cut Jurassic and oldest volcanic-sedimentary rocks. Plutonic composition is granodiorite to granite. The main minerals consist of quartz, alkali feldspar, plagioclase and ferromagnesian minerals are biotite and amphibole. It the most ferromagnesian minerals change to chlorite and secondary minerals. One of the features of this intrusive is its physical elasticity and minerals crunch ability in NW-SE along with the explosion of zagros during the Alpine Orogeny. Geochemically these rocks are of the subalkaline, calc-alkaline series, metaluminous, and display typical features of magnesium I-type granites. The south Tiran granitoid rocks are characterized by enrichment in large ion lithophile elements (LILE) such as Rb, Ba, K, Ce and depletion in high field strength elements (HFSE) such as Y, Nb and Zr. The conderite normalized REE patterns are characterized by moderate to high LREE enrichment [(La/Yb) N = 7.70–10.90] and unfractionated HREE [(Gd/Yb) N N = 1.59 - 2.07]. Granodiorites with the least fractionated HREE and has a negative of Eu anomalies (Eu/Eu*=0.38-0.53) are indicative of feldspar involvement during fractionation and/or melting. This granitoid magma involves low grade partial melting of metasomatic mantle wedge or oceanic plate. Continental crust plays an important role in magma arrangement. The Tiran granitite has mineralogical field and geochemical characteristics typical of volcanic arc granites related to an active continental margin. Probably, the mass is the result of the subduction of Neotetis oceanic plate below the Lut micro continent and this oceanic residual plate during Jurassic and late time.

Key words: Tiran granitoid, I-type granite, Jurassic, Calc-Alkaline.

INTRODUCTION

The studied area is located approximately in 65 km to the west of Isfahan and Tiran to the south with longitude of 51° 4' to 50° 55' and latitude of 33° 32' to 40' (Fig .1).the targeted region banks on zayande Roud river (Tillman, *et al.*, 1981). There is a fissured part along the southern part of Sanandaj - Sirjan which protrudes a bit. This hump is mostly made of volcanic as well as deposited recurrence (Ghasemi, 1385; Zahedi, 1978). This region encircles part of Shahre Kord - Dehsard (Arfania and Shahriari, 2009).

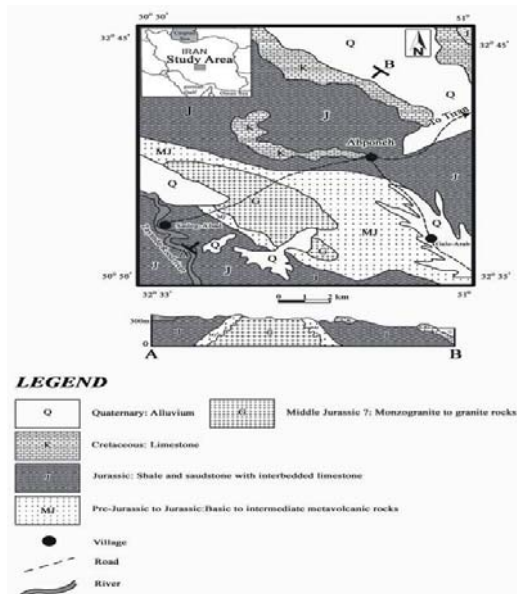


Fig. 1: Geological map of the study area (Ghasemi *et al.*, 1385).

Corresponding Author: Marziyeh Mehranfar, Petrology department, Islamic Azad University, Khorasgan Branch, Isfahan, Iran.

Green schist facies metamorphism in the affected area is located (Nasr Esfahani, Aly Khan, 1371). The overall trend of the outcrops of the platoon, North West - South East, parallel to the Zagros Mountains. Tectonic intrusion under pressure, mainly in South West - North East shows the deformation and small punctures. Dikes associated with the rock mass around metabasalt are off. By dikes of mafic rocks include their mass and has been discontinued.

Research Technique:

During visits to the field of parts alteration to the mass of granite, 63 rock samples were taken after the 40 thin sections and study them with a polarizing microscope, 7 samples using ICP-MS analyze isotope oxygen-stable, respectively, in the laboratory Acme Labs in Canada and Cornell University USA (Tables 1 and 2) and 5 samples using XRF in the company's Scientific research, University of Isfahan, analysis of major and minor, were (Tables 3 and 4), the three thin sections with a microscope sample using SEM studied mineralogy .

Table 1: Analysis of chemical elements (% Wt) in the south Tiran samples (ICP-MS method).

	A-54	A-55	A-56	A-57	A-59	A-60	A-25
SiO ₂	72.1	72	72.2	69.8	70.5	65.6	70
Al ₂ O ₃	12.1	12.59	13.51	13.38	14.5	14.19	14.12
Fe ₂ O ₃	3.12	2.3	2.8	4.72	3.66	7.88	3.42
CaO	0.71	0.83	1.2	1.26	1.47	2	2.07
MgO	1.53	0.63	1.09	2.5	1.28	3.75	1.14
Na ₂ O	6.88	3.94	3.83	3.8	5.71	3.42	3.55
K ₂ O	0.18	4.37	4.12	2.48	1.01	0.99	4.17
TiO ₂	0.43	0.25	0.32	0.62	0.44	1.01	0.44
MnO	0.03	0.03	0.04	0.05	0.04	0.08	0.04
P ₂ O ₅	0.19	0.15	0.21	0.21	0.19	0.26	0.19
LOI	2.7	2.9	0.71	1.15	1.25	0.85	0.87
Total	97.26	97.08	99.33	98.82	98.79	99.17	99.14
Mg#	49.44	35.36	43.83	51.46	41.07	48.73	40.08
ACNK	0.77	0.8	0.84	0.96	0.9	1.11	0.81
(Nb/Zr)N	33.36	37.81	48.92	69.42	48.9	118.16	49.49
EU/EU*τ	0.43	0.38	0.44	0.39	0.47	0.53	0.42
(La/Yb)N	7.7	9.96	9.07	8.92	10.4	7.74	1.17
(Gd/Yb)N	1.59	2.11	2.03	2.02	1.96	1.64	2.07
τ	12.11	35.03	30.08	15.4	20.03	10.68	23.82
FM	0.54	0.68	0.6	0.52	0.62	0.55	0.63
MALI	6.35	7.49	6.74	5.02	5.25	2.41	5.65
K ₂ O/Na ₂ O	0.03	1.11	1.08	0.65	0.18	0.29	1.17
Σ	1.71	2.38	2.16	1.47	1.64	0.86	2.21
δ ¹⁸ O	3.9	4.53	9.71	7.02	3.17	1.78	6.85

Table 2: Results of chemical analysis of samples of South Tiran (using ICP-MS).

	Unit	A-54	A-55	A-56	A-57	A-59	A-60	A-25
Ba	ppm	24	1190	809	344	201	183	1141
Ce	ppm	76.31	51.49	56.86	81.41	83.67	98.32	67.77
Co	ppm	4.4	3.7	5.5	6.6	6.6	19.8	5.6
Cr	ppm	28	17	24	31	24	71	23
Cs	ppm	0.5	0.6	0.8	0.8	0.4	0.5	0.9
Cu	ppm	4.53	8.08	14.09	3.97	10.93	14.63	12.45
Dy	ppm	6.4	4.0	4.9	6.5	5.8	7.4	5.0
Er	ppm	3.5	2.1	2.4	3.1	2.7	4.0	2.5
Eu	ppm	0.9	0.6	0.8	0.9	1.0	1.4	0.8
Ga	ppm	14.60	14.98	16.82	18.63	19.15	15.96	13.31
Gd	ppm	5.8	4.5	5.1	6.6	5.9	7.4	5.2
Hf	ppm	0.27	0.15	0.14	0.19	0.18	0.13	0.15
Ho	ppm	1.3	0.8	0.9	1.2	1.1	1.4	1.0
La	ppm	33.5	25.4	27.2	34.8	37.4	41.7	32.7
Rb	ppm	6.7	82.1	86.6	62.9	30.9	27.6	86.4
Sr	ppm	64	181	174	94	209	183	158
Y	ppm	32.6	20.8	23.9	31.3	28.8	37.9	25.0
Zr	ppm	5.2	2.7	2.5	3.2	3.3	2.0	3.1
Nb	ppm	11.76	6.92	8.29	15.06	10.94	16.02	10.40
Th	ppm	14.2	10.0	11.9	15.4	14.6	15.2	13.7
Pb	ppm	2.01	12.05	12.85	7.54	11.89	4.29	27.74
Zn	ppm	28.9	26.7	34.3	43.0	46.9	59.0	34.0
Ni	ppm	12.2	6.7	10.0	14.9	10.8	37.3	11.4
V	ppm	45	30	36	72	50	151	48
Ta	ppm	0.7	0.4	0.5	0.8	0.6	0.8	0.6
U	ppm	1.1	1.1	1.2	1.2	1.1	1.8	1.2

W	ppm	1.0	0.8	1.0	1.2	1.0	0.7	1.1
Sn	ppm	3.7	2.5	2.8	4.2	3.7	2.7	3.5
Mo	ppm	1.18	0.58	0.24	0.24	0.15	0.53	0.48
Pr	ppm	8.1	6.2	6.8	8.7	9.0	10.5	7.8
Nd	ppm	35.2	25.9	27.2	36.6	38.5	44.2	33.3
Sm	ppm	6.4	4.8	5.6	7.0	6.7	8.0	5.9
Tb	ppm	1.0	0.7	0.8	1.0	0.8	1.2	0.8
Tm	ppm	0.5	0.2	0.3	0.4	0.3	0.5	0.3
Yb	ppm	2.9	1.7	2.0	2.6	2.4	3.6	2.0
Lu	ppm	0.4	0.2	0.3	0.3	0.3	0.5	0.3
Tl	ppm	0.258	0.148	0.193	0.373	0.263	0.605	0.266

Table 3: amounts of oxides of the basic rocks (% Wt) – XRF Method.

Sample	A11	A13	A13C	A17	A19B	I 20	L25A
SiO ₂	72.1	71.17	72.14	72.65	69.06	73.74	66.03
Al ₂ O ₃	13.23	13.96	13.96	14.09	14.21	12.8	13.84
Fe ₂ O ₃	8.24	2.96	2.95	3.06	4.97	1.28	3.67
CaO	0.19	1.52	1.05	0.45	0.99	0.79	2.35
MgO	1.088	1.1	0.59	2.03	2.82	0.48	1.58
Na ₂ O	0.184	3.18	3.79	5.13	4.19	2.77	3.46
K ₂ O	4.06	4.37	4.95	1.5	1.7	6.04	3.85
TiO ₂	0.141	0.49	0.49	0.44	0.71	0.22	0.54
MnO	0.021	0.05	0.02	0.03	0.04	0.01	0.04
P ₂ O ₅	0.061	0.24	0.18	0.25	0.28	0.26	0.2
LOI	0.12	0.62	0.61	0.23	0.62	1.25	3.42
Total	99.8	99.8	100.9	99.99	99.79	99.7	99.1

Table 4: Concentrations of minor and rare elements in the rocks (ppm) - XRF Method.

Sample	A11	A13	A13C	A17	A19B	I 20	L25A
Ba	6	5	9	8	7	8	12
Co	166	99	80	130	136	88	99
Ho	6	3	2	6	1	4	3
La	130	142	132	72	51	137	101
Rb	25	173	172	102	130	147	165
Sr	26	37	30	36	0	35	380
Y	161	187	114	158	251	118	230
Zr	11	12	7	11	14	5	11
Nb	9	12	10	11	13	10	16
Zn	9	13	8	13	22	8	15

Table 5: Results of intrusive checking of plagioclase in southern Tiran.

Sample	PL-1	PL-2	PL-3	PL-4	PL-5	PL-6	PL-7
Mineral	Fel	Fel	Fel	Fel	Fel	Fel	Fel
SiO ₂	56	53	44	60	65	53	62
TiO ₂			6.4	0.28	0.57		0.57
Al ₂ O ₃	28.6	31.23	25.99	26.93	25.37	31.23	25.37
FeO	0.95	2.42	5.19	0.35	1.05	2.42	1.05
CaO	4.78	2.77	12.48	1.81	1.93	2.77	1.93
Na ₂ O	8.31	7.01	5.43	8.27	4.8	7.01	4.8
K ₂ O	0.93	3.56	0.44	1.53	0.96	3.56	3.88
Total	99.57	99.99	99.93	99.17	99.68	99.99	99.6
Si	2.53	2.42	2.11	2.68	2.83	2.42	2.76
Al	1.52	1.68	1.47	1.42	1.3	1.68	1.33
Ti	0	0	0.23	0.01	0.02	0	0.02
Fe ²⁺	0.04	0.09	0.21	0.01	0.04	0.09	0.04
Ca	0.23	0.14	0.64	0.09	0.09	0.14	0.09
Na	0.73	0.62	0.51	0.72	0.41	0.62	0.41
K	0.05	0.21	0.03	0.09	0.05	0.21	0.22
Cations	5.10	5.15	5.19	5.01	4.73	5.15	4.87
X	4.05	4.10	3.81	4.10	4.15	4.10	4.11
Z	1.05	1.05	1.38	0.90	0.59	1.05	0.77
Ab	71.9	64.4	43.1	80.4	73.9	64.4	57
An	22.8	14	54.6	9.8	16.4	14	12.7
Or	5.3	21.5	2.3	9.8	9.7	21.5	30.3

Table 6: Plagioclase present in masses of southern Tiran.

Sample	Anorthite (%)	Albite (%)	Orthoclase (%)
PL-1	22.8	72.3	5.0
PL-2	14.6	64.6	21.9
PL-3	54.7	43.6	2.6
PL-4	10.1	80.9	10.1
PL-5	16.4	74.5	9.1
PL-6	14.6	64.6	21.9
PL-7	12.3	56.2	30.1

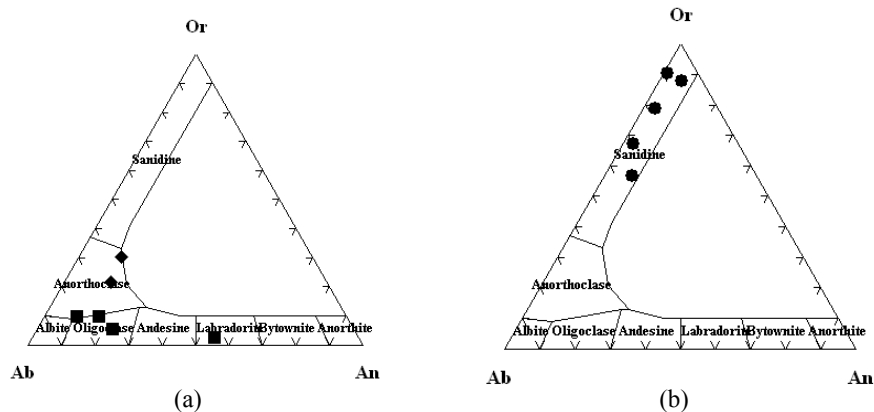
Table 7: Results in intrusive checking of orthoclase present in southern Tiran.

Sample	Or-1	Or-2	Or-3	Or-4	Or-5
Mineral	Fel	Fel	Fel	Fel	Fel
SiO ₂	12.79	20	60	67	52
Al ₂ O ₃	6.40	25.96	23.62	20.81	25.11
FeO	0.87	29.37	0.87	0.61	1.03
CaO	0.95	1.41	0.98	0.5	0.25
Na ₂ O	2.3	0.65	5.4	1.31	1.22
K ₂ O	5.6	15.64	18.43	8.93	19.64
Total	28.90	93.03	109.3	99.16	99.25
Si	2.30	1.31	2.66	3.00	2.55
Al	1.36	2.00	1.23	1.10	1.45
Fe ²⁺	0.13	1.60	0.03	0.02	0.04
Ca	0.18	0.10	0.05	0.02	0.01
Na	0.80	0.08	0.46	0.11	0.12
K	1.29	1.30	1.04	0.51	1.23
Cations	6.06	6.39	5.48	4.77	5.40
X	3.66	3.3	3.98	4.09	4.00
Z	2.40	3.09	1.59	0.67	1.40
Ab	35.3	5.5	29.9	17.6	8.5
An	8.1	6.7	3	3.7	1
Or	56.6	87.8	67.1	78.7	90.5

Petrography:

Generally, the average seed mass and texture (remnants of granular tissue) are. Small punctures in the general area have all the geological outcrops. Large feldspar crystals with combination of alkaline minerals and microcline are with abundant quartz region in the rocks. These crystals are partly altered to clay minerals. In thin section, quartz crystals with amorphous, toothed margins and turn off the wave are detected and is severely lacking. The composition of plagioclase with albite and oligoclase twin deformation less than alkaline feldspar are found in rocks. These minerals are serisit as the mineral composition is difficult to distinguish them (Fig 4 a). Microprobe analysis and structural formula and the final member of this mineral in the tables (5, 6) are given. Figure Ab -An-Or (Deer *et al.*, 1991), almost more samples of albite are formed in the range of chemical plagioclase (Fig 2 a).

Sphene and zircon is as accessory minerals in the rocks. Lanite with optical properties similar to small amounts of epidote is observed. Combining zoisite, epidote, and clinozoisite scattered along fractures (Fig. 4d). Muscovite is as secondary mineral and still recrystallization serisit and phenzhte optical characteristics of the symptoms.

**Fig. 2:** (a) The classification of plagioclase (Deer *et al.*, 1991), (b) The classification of orthoclase (Deer *et al.*, 1991).

Nomenclature and Geochemical Properties:

Average amount of SiO_2 , Al_2O_3 , MgO , CaO , Na_2O would be 70.65, 13.61, 1.54, 1.21, 3.84, 3.13. All samples contain high amount of Si and K. Granitites are a ubiquitous component of the crust. They have crystallized from magmas that have compositions at or near a eutectic point (or a temperature minimum on a cotectic curve). Magmas will evolve to the eutectic because of igneous differentiation, or because they represent low degrees of partial melting. Fractional crystallization serves to reduce a melt in iron, magnesium, titanium, calcium and sodium, and enrich the melt in potassium and silicon - alkali feldspar (rich in potassium) and quartz (SiO_2), are two of the defining constituents of granite. This process operates regardless of the origin of the parental magma to the granite, and regardless of its chemistry. However, the composition and origin of the magma which differentiates into granite, leaves certain geochemical and mineral evidence as to what the granite's parental rock was. The final mineralogy, texture and chemical composition of granite is often distinctive as to its origin. For instance, granite which is formed from melted sediments may have more alkali feldspar, whereas granite derived from melted basalt may be richer in plagioclase feldspar. It is on this basis that the modern "alphabet" classification schemes are based (Barbarin, 1999).

Magma Origin:

The granitoid indigenous to southern Tiran, according to petrologic diagrams (Vigneresse, 2004; Whalen *et al.*, 1999), indicate same properties much like I-TYPE granite. (Frost *et al.*, 2001) The Granite Belt, Australia Lakhlan folded according to the two main elements, magnesium and division were Hndar. Magnesium group, including both type I or S-type granites of A-type groups is Hndar. The samples studied in the range of granite and magnesium are type I, also of granite and granite Kordylera America according to the FM and Hndar divided magnesium. Kordylera been striped of granite in the region are shown (Fig. b6). Given the above examples, often stones with less than 70% SiO_2 < a class are replaced with magnesium. According to this diagram, the samples within the study area with granite Kalkv magnesium are alkaline (Fig. c6). Graphs Petrogenesis (Altherr, 2000; Patino, 1993), indicating the origin of amphibolites to metagraywak (Fig. 7).

Isotope Oxygen:

Stable isotopes are meant to determine the origin of magma and solutions and in certain circumstances can be used to determine the temperature of the solution (Fig. a3) in the range of oxygen isotope variation is plotted. Granite oxygen isotopic ratios usually vary from 6 to 8, the changes in oxygen isotopes of granitoid 1 / 78 to 9 / 71 is variable.

Oxygen isotope studies of the S-type granites, and I have been plotted in the graph in Figure 3 b. Oxygen isotopes in the S-type granites in the range of 10 to 13 and I-type granites in the area varies from 6 to 10. The average oxygen isotope S-type granites are about 8 to about 12 and I-type granites (Fig. 3b). As the back of the studied granites are I-type granites in the area. This confirmed the possibility of forming a volcanic arc environment in the Jurassic.

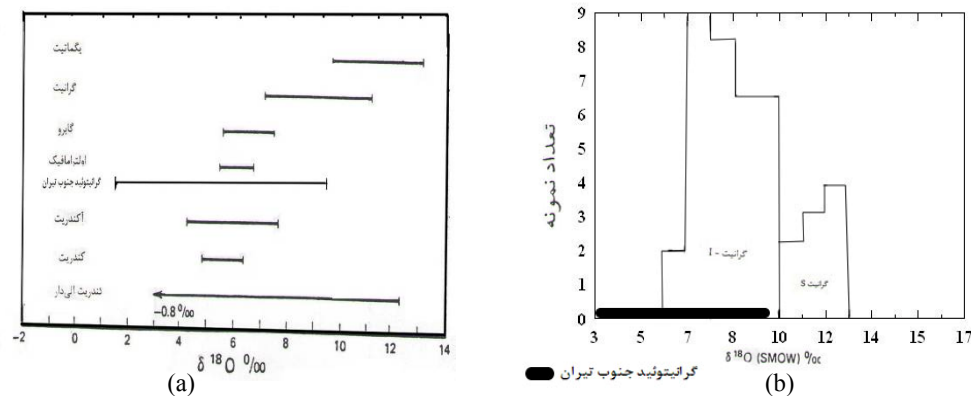


Fig. 3: (a) the range of variations of oxygen isotopes in igneous rocks and granitoid showing location of West, (b) Comparison of oxygen isotopes in the range of S-type granites (Davidson, 1986).

Spider Type Diagram:

To examine patterns, REE_S usually uses normalized charts (Taylor, *et al.*, 1985), this diagram (Fig. a 8) shows a trend almost uniformly flat, and the overall pattern subtraction, not the distribution of elements HREES offers (1/59- 2 / 07 (Gd / Yb)_N =), is the movement supports LREES enriched and subtracted from the show (7/70-10/90 (La / Yb)_N =). This circumstances indicate that fractionation of these elements, Eu negative anomaly

of the show (0/38-0/53 Eu/Eu \neq). Feldspar separation of the negative Eu anomaly is the origin of the felsic melts (Taylor *et al.*, 1985). in the form c 8 Changes in trace elements than many of their Conderite normalized is (Taylor, *et al.*, 1985) and negative anomalies, and distinct from Rb, Ni, Sr, Zr and P, as well as anomalies, positive Tb, La, Ba and Ce shows that certain granitoid and (Parada *et al.*, 1999) stated that the enrichment of

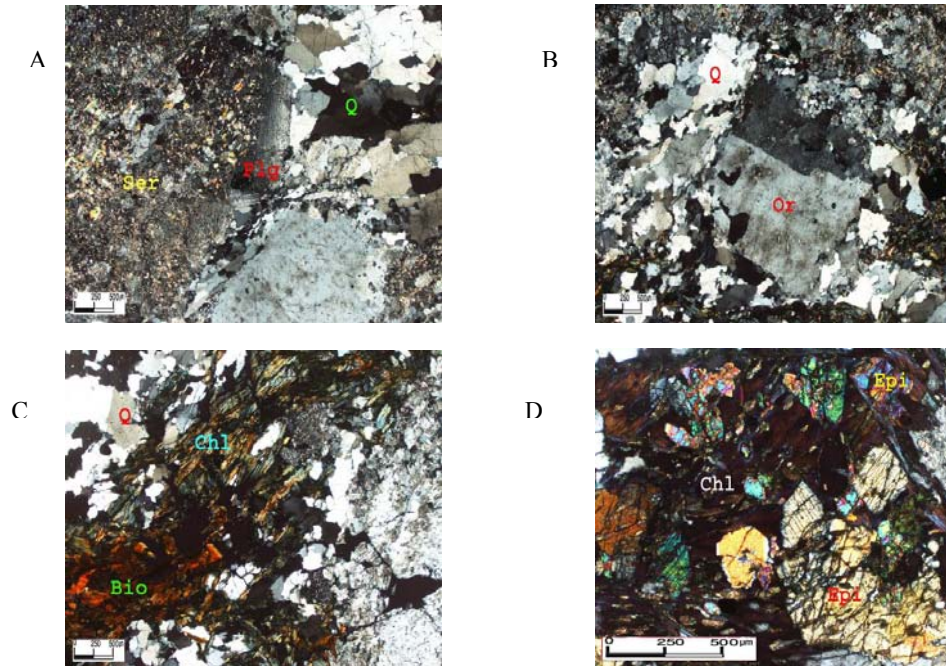


Fig. 4: Macroscopic view of plutonic intrusive.

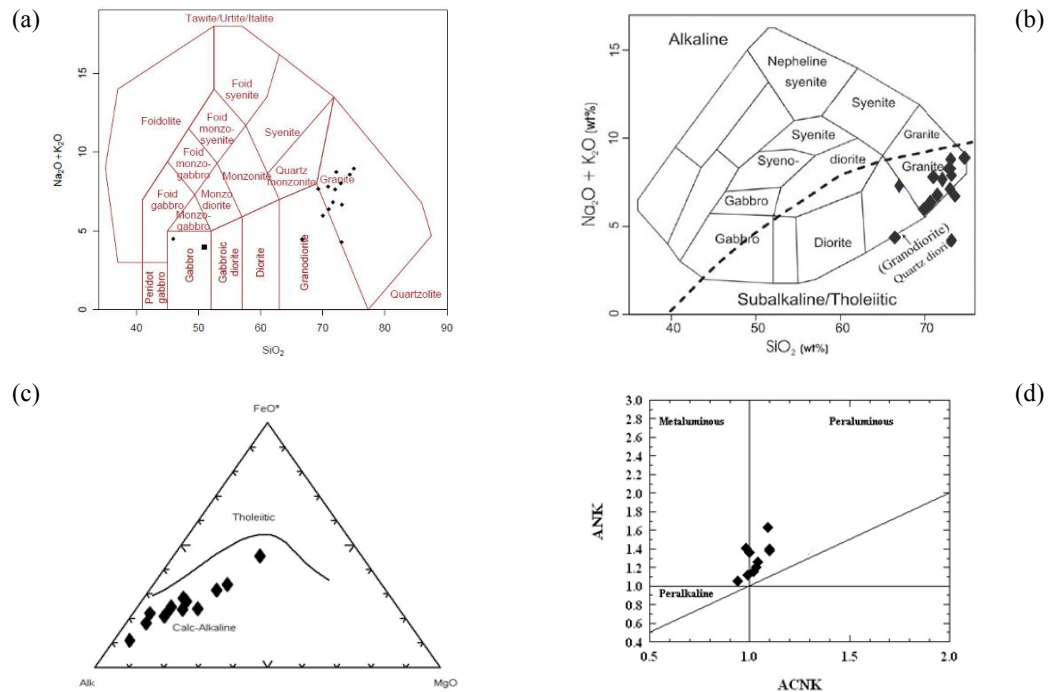


Fig. 5: Classification of the igneous rocks: (a) alkali versus silica diagram (Middlemost, 1985), (b) alkali versus silica diagram (Cox *et al.*, 1979; Wilson, 1989), (c) AFM diagram (Irvine and Baragar, 1971), and (d) plot of A/NK versus A/CNK [A/NK = molar $\text{Al}_2\text{O}_3/(\text{Na}_2\text{O}+\text{K}_2\text{O})$ and A/CNK = molar $\text{Al}_2\text{O}_3/(\text{CaO} + \text{Na}_2\text{O}+\text{K}_2\text{O})$] (Maniar and Piccoli, 1989).

many elements LREEs be due to partial melting of small rocks or a source relatively rich in the alkaline-related areas of subduction is (Parada *et al.*, 1999), pattern subtraction, not HREEs indicates that magma out of the field stability of garnet produced, while the anomaly of negative Eu and Sr represents the stability of plagioclase in the source can be in the form b 8 samples of the primitive mantle normalized that fluctuations in HREE large and anomalies indicate the enrichment of REE elements may reflect the partial melting of primitive mantle or the enrichment of these may be controlled by partial melting. La, Pr, Eu, Tm and negative anomaly for Ce, Ho, Yb show a positive anomaly Zr concentration is intense. Rb, Th, Nb and Ba anomalies are positive but Cr and Ni has a negative anomaly. The elements are enriched to nearly 100 times.

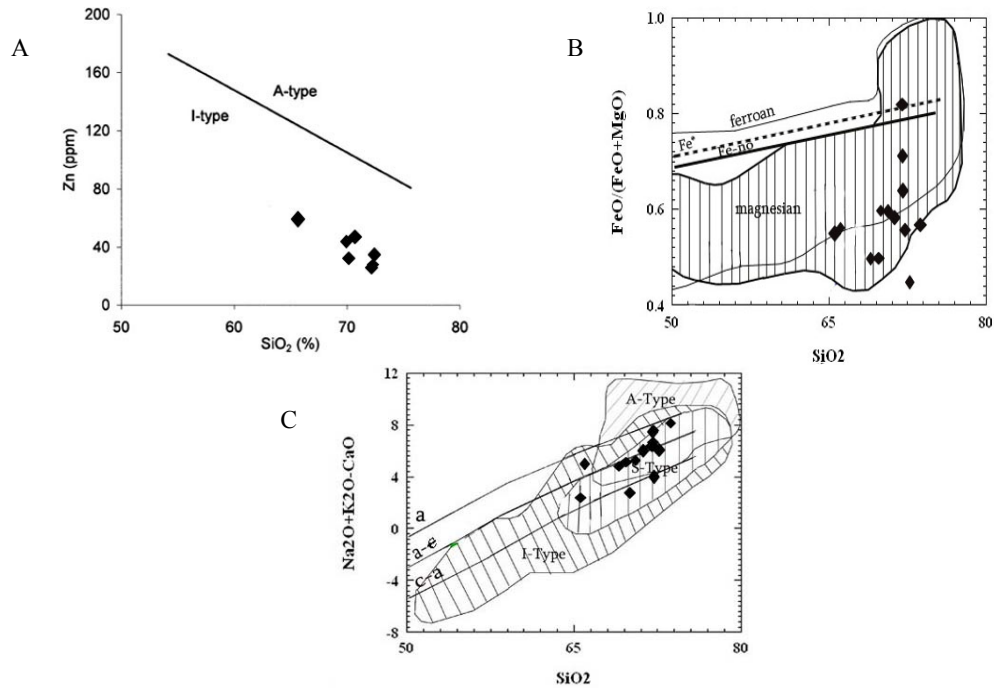


Fig. 6: (a) Selected geochemical diagrams showing the I-type (Vignersse, 2004), (b) FeO/(FeO+MgO) vs. Wt% SiO₂ and (c) Na₂O+K₂O-CaO vs. Wt% SiO₂ plots showing the compositions range for the rocks from study area (Frost *et al.*, 2001).

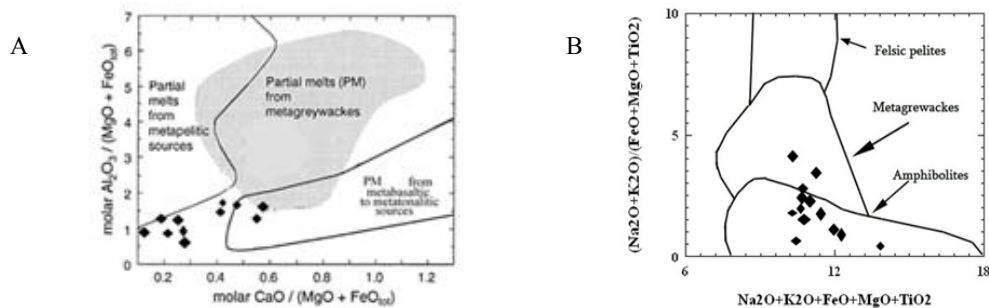


Fig. 7: (a) diagrams Molar Al₂O₃/(MgO+FeO) vs Molar CaO/(gO+FeO) (Altherr, 2000), (b) Astaneh granitoids plotted on the (Na₂O + K₂O)/FeO + MgO + TiO₂ vs. Na₂O + K₂O + FeO + MgO + TiO₂ (Patino, 1993).

Tectonic Setting:

The tectonic discrimination diagrams of (Pearce and Cann, 1983) may help to determine the geologic setting, although they must be used with caution as they may represent the formation conditions of the protoliths rather than those of the derived magmas. Most rocks plot in the volcanic arc (VAG) (Fig. 9).

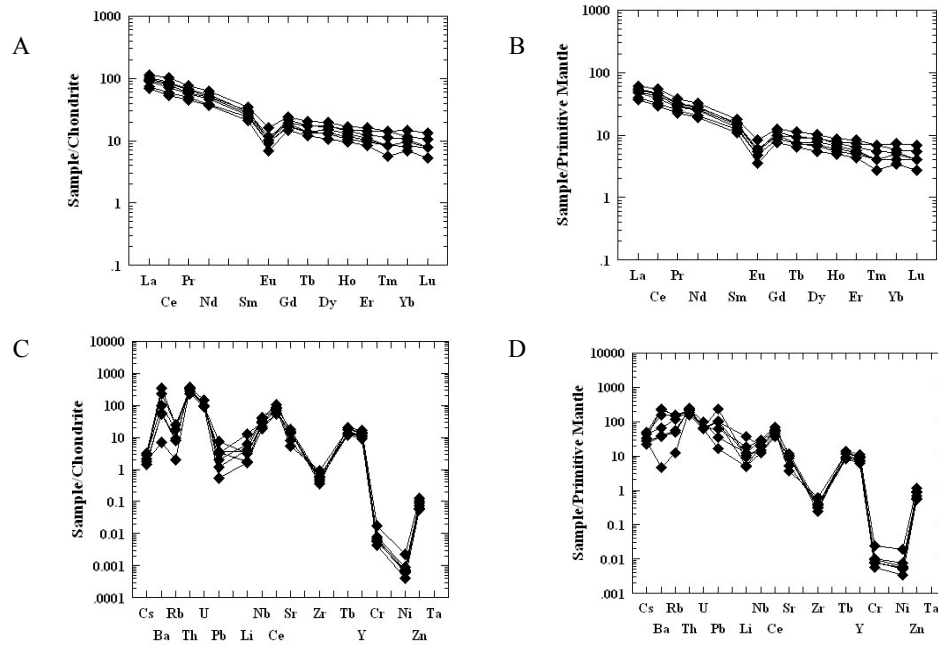


Fig. 8: (a–b) Conderite and Primitive mantle-normalized rare earth element abundances. (c–d) Conderite and Primitive mantle-normalized trace element abundances. The normalizing values are from (Taylor and McLennan, 1985).

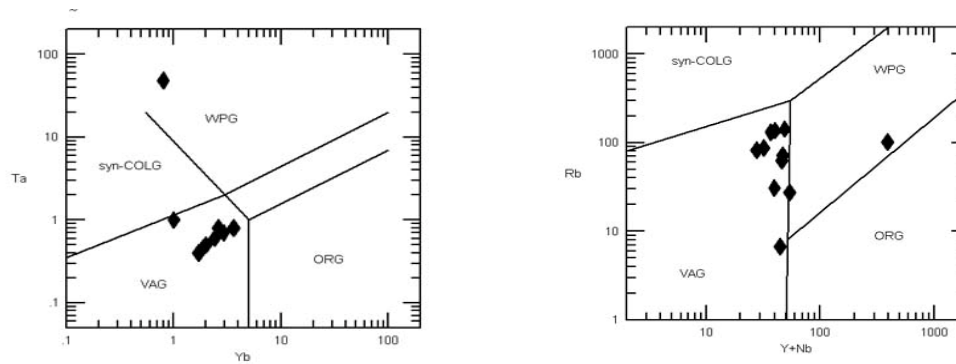


Fig. 9: Granite distinguishing diagrams based on (a) Ta vs. Yb, (b) Rb vs. Y + Nb (Pearce and Cann, 1983) that the volcanic arc granites (VAG), the collision granites (syn-COLG), within this convention granites (WPG) and ocean ridge granites (ORG) shows.

Although the plot and granitites (Batchelor and Bowden, 1985) in the range of granite groups, samples, mainly in southern Tiran associated with the arc belongs (Fig. b-d10). also, the high Th / Yb and La / Yb (10-100) (Fig d10) and continent-arc felsic magmas want to emphasize is given to the mass (Condie, 2002). as noted in the chart, Th / Ta - Yb form (Fig. b8) (Liegeois Black, 2007), the ratio of logarithmic Th / Yb versus Ta / Y (Schandl and Gorton, 2002), indicate the formation of these masses in the range of margins on a continent (Fig. c10).

Conclusion:

Periods during the Mesozoic and Cenozoic granitic intrusive in Sanandaj - Sirjan are present (Sabzeyi Yi, Mosayebi, Davoodzadeh and Difenbach, 1987). Located in Sanandaj - Sirjan inner Zagros orogenic metamorphism in the West that Iran is closing the Tethys Ocean in the Cretaceous of young Arab with Iran on the plate there is created (Mohajjel and Fergusson, 2000; Alavi, 1994).

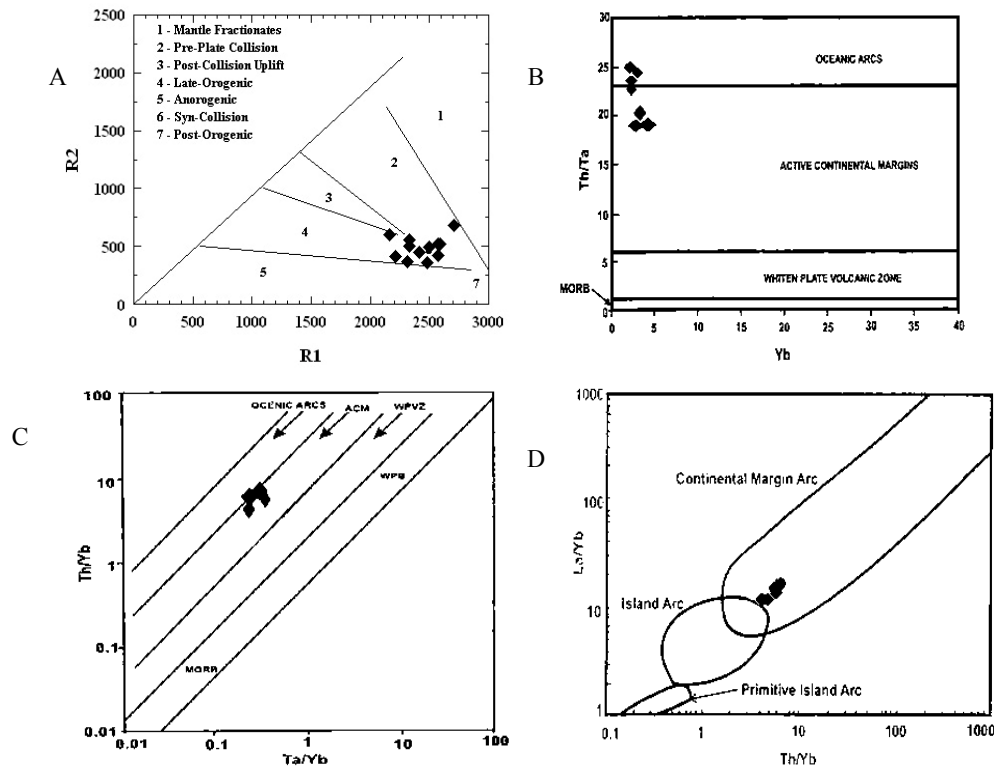


Fig. 10: (a) R1–R2 major element plot (Batchelor and Bowden, 1985), (b) Th/Ta versus Yb (Liegeois and Black, 2007), (c) Th/Yb versus Ta/Y (Schandl and Gorton, 2002), (d) diagram Th/Yb-La/Yb (Condie, 2002).

Most intrusive rocks of Middle Jurassic age - in the Paleocene zone, in areas of Hamadan Boroujerd to have influence. Characteristics of granitoid looking all along the North West - South East, and shows the influence of tectonic pressure is transformed them (Mohajjel and Fergusson, 2000; Ghasemi Valizadeh and 0.1372). The wisdom of the continent's central Rift Neotetis punctures in Upper Carboniferous - Early Permian has occurred (Babaie *et al.*, 2003). The Upper Triassic - Lower Jurassic present to the central Iranian micro-continent was observed (Reuter *et al.*, 2007; Shafaii-Moghadam *et al.*, 2007). (Arfania and Shahriari, 2009) Based on the specific characteristics of land Shahrekord ocean basin between the first and second Neotetis presented. According to this model in the Late Triassic - Lower Jurassic began with the closure of primary to the central Iranian micro-continent, and land occur in Shahrekord - Dehsrd North East of the Arabian plate margins - from African and a back-arc basin evolution, volcanic are to be found.

REFERENCES

- Alavi, M., 1994, Tectonics of the Zagros Orogenic belt of Iran: New Data & Interpretations, *Tectonophysics*, 229: 211-238.
- Altherr, R., A. Holl, E. Hegner, C. Langer and H. Kauzer, 2000. High Potassium, Calc-Alkaline I-type Plutonism in the European, *Lithos*, 50: 51-73.
- Arfania, R., S. Shahriari, 2009. Role of southeastern Sanandaj-Sirjan Zone in the tectonic evolution of Zagros Orogenic Belt, Iran. *Journal of Island Arc*, 18: 555-576.
- Babaie, H.A., A.M. Ghazi, A. Babaei, R. Duncan, J. Mahony and A. Hssanipak, 2003. New Ar-Ar age, isotopic, and geochemical data for basalts in the Neyriz ophiolite, Iran. *Geophysical Research Abstracts*, 5(12): 899.
- Barbarin, B.A., 1999. Review of the relationship between granitoid types, their origins and geodynamic environments, *Lithos*, 46: 605-626.
- Batchelor, R.A. and P. Bowden, 1985. "Petrogenetic interpretation of granitoid rock series uses multicaticonic parameters", *Chem. Geo.*, 48-55.
- Condie, K.C., 2002. Geochemical changes in basalts and andesites across the Archean-Proterozoic boundary: Identification and significance, *Lithos.*, 23: 1-18.
- Cox, K.G., J.D. Bell and R.J. Pankhurst, 1979. The interpretation of igneous rocks. George Allen and Unwin, 45.

- Davidson, J.P., 1986. Isotopic and trace element constraints on the petrogenesis of subduction related lavas from Martinique Lesser Antilles. *Journal of Geophysical Research*, 91: 5943-5962.
- Davoudzadeh, M. and K. Diefenbach, 1987. Contribution to the Paleogeography of upper Paleozoic of Iran. Stuttgart, 175: 121-146.
- Deer, W.A., R.A. Howie, J. Zussman, 1991. "An introduction to the Rock Forming Minerals", 17th Longman, edition, pp: 528.
- Frost, B.R., C.G. Barends, W.J. Collins, R.A. Arculus, D.G. Ellis and C.D. Froat, 2001. A Geochemical Classification for Gabbroic Rocks, *J. of Petrol.*, 11: 2033-2048.
- Ghasemi Haj-Hosseini, A., M. Hosseini, 1385. Chadegan quadrangle geological maps (scale 1:100000). Geological Survey Ghasemi Valizadeh and 0.1372. Granitoids of Bvyyyn - Miandasht Journal of Earth Sciences, the GSI.
- Irvine, T.N. and W.R.A. Baragar, 1971. A guide to the chemical classification of the common volcanic rocks. *Can. J. Earth Sci.*, 8: 523-548.
- Liegeois, J.P. R. Black, 2007, Alkaline magmatism subsequent to collision in the pan-African belt of the Adrar des Iforas. In: Fitton JG, Upton BGJ (eds) Alkaline igneous rocks. *Geol. Soc. London, Special Publication*, 30: 381-401.
- Maniar, P.D. and P.M. Piccoli, 1989. Tectonic discrimination of Granitoids, *Geological Society of American Bulletin*, 101: 635-643.
- Middlemost, E.A.K., 1985. Magmas and magmatic rocks, An introduction to igneous petrology. Longman Groupuk, pp: 73-87.
- Mohajjel, M., C.L. Fergusson, 2000. Dextral transpression in Late Cretaceous Continental Collision, Sanandaj-Sirjan zone, Western Iran. *Journal of structural Geology*, 22: 1125-1139.
- Nasr Esfahani, and Aly Khan, 1371. Open pit mine storing the remaining terms of weeding, the internal report Anjireh mining company.
- Parada, M.A., J.O. Nystrom and B. Levi, 1999. Multiple source for the Coastal Batholith of Central Chile: geochemical and Sr-Nd isotopic evidence and tectonic implication. *Lithos*, 46: 505-521.
- Patino D.A.E., 1993. "Titanium substitution in biotite: An empirical model with applications to thermometry, O₂ and H₂O barometries, and consequences for biotite stability, chemical Geology, 108: 133-162.
- Pearce, J.A. and J.R. Cann, 1983. Tectonic setting of basic volcanic rocks determined using trace element analyses. *Earth Planet. Sci. Lett.*, 19: 290-300.
- Reuter, M., E. Pillerw, M. Harzhauser *et al.*, 2007. The Oligo-/Miocene Qom Formation (Iran): Evidence for an early Burdigalian restriction of the Tethyan Seaway and closure of its Iranian gateways. *International Journal of Earth Science*, 98: 627-650.
- Sabzeji, Yi, Mosayebi, 0.1369. Geodynamics model transformation zone of Sanandaj - Sirjan and broken edges of the Zagros, the ninth meeting of Earth Sciences, Geological Survey of Iran.
- Schandl, E.S., M.P. Gorton, 2002. Application of high field strength elements to discrimination tectonic setting in VMS environments. *Econ. Geol.*, 97: 629-642.
- Shafaii-Moghadam H., M. Rahgoshay and H. Whitechurch, 2007. The Naien-Baft ophiolites: An evidence of back-arc basin spreading in the active margin of the Iranian continent. *Geophysical Research Abstracts*, 9: 791.
- Taylor, S.R. and S.M. McLennan, 1985. The continental crust: its composition and evolution. Blackwell, Oxford.
- Tillman, J.E., A. Poosti, S. Rossello and A. Eckert, 1981. Structural evolution of Sanandaj-Sirjan ranges near Esfahan, Iran. *American Association Petroleum Geol Ologists Bulletin*, 65: 674-687.
- Vigneresse, J.L., 2004. A new paradigm for granite generation. *Trans, Royal Soc. Edinbu. Earth Sci.*, 95: 11-22.
- Whalen, J.B., K.L. Currie and B.W. Chappell, 1999. "A-type Granites, geochemical characteristics, discrimination and petrogenesis. , *Contrib. Min. Pet.*, 95: 407-419, 605-626.
- Wilson, M., 1989. Igneous petrogenesis, Unwin Hyman London. 466p.
- Zahedi, M., M. Samadi, M. Tavvysyan Sh., 1978. Of geological maps (scale 1:250000), Geological Survey of Iran.